SCIENTIFIC REPORTS

OPEN

SUBJECT AREAS:
EXPERIMENTAL MODELS OF DISEASE
CHRONIC INFLAMMATION

Received
24 January 2014

Accepted
15 May 2014

Published
4 June 2014

Correspondence and requests for materials should be addressed to K.N. (narusek@dpc.agu.ac.jp)

Periodontitis-activated monocytes/macrophages cause aortic inflammation

Shin-ichi Miyajima[1], Keiko Naruse[2], Yasuko Kobayashi[2], Nobuhisa Nakamura[2], Toru Nishikawa[1], Kei Adachi[1], Yuki Suzuki[1], Takeshi Kikuchi[1], Akio Mitani[1], Makoto Mizutani[3], Norikazu Ohno[3], Toshihide Noguchi[1] & Tatsuaki Matsubara[2]

[1]Department of Periodontology, School of Dentistry, Aichi Gakuin University, 2-11 Suemori-dori, Chikusa-ku, Nagoya, Aichi, 464-8651, Japan, [2]Department of Internal Medicine, School of Dentistry, Aichi Gakuin University, 2-11 Suemori-dori, Chikusa-ku, Nagoya, Aichi, 464-8651, Japan, [3]Department of Oral Anatomy, School of Dentistry, Aichi Gakuin University, 1-100 Kusumoto-cho, Chikusa-ku, Nagoya, Aichi, 464-8650, Japan.

A relationship between periodontal disease and atherosclerosis has been suggested by epidemiological studies. Ligature-induced experimental periodontitis is an adequate model for clinical periodontitis, which starts from plaque accumulation, followed by inflammation in the periodontal tissue. Here we have demonstrated using a ligature-induced periodontitis model that periodontitis activates monocytes/macrophages, which subsequently circulate in the blood and adhere to vascular endothelial cells without altering the serum TNF-α concentration. Adherent monocytes/macrophages induced NF-κB activation and VCAM-1 expression in the endothelium and increased the expression of the TNF-α signaling cascade in the aorta. Peripheral blood-derived mononuclear cells from rats with experimental periodontitis showed enhanced adhesion and increased NF-κB/VCAM-1 in cultured vascular endothelial cells. Our results suggest that periodontitis triggers the initial pathogenesis of atherosclerosis, inflammation of the vasculature, through activating monocytes/macrophages.

Cardiovascular disease is the number one cause of death in the world. An estimated 17.3 million people die from cardiovascular disease, representing 30% of all global deaths[1]. Atherosclerosis, which is the most important contributor to cardiovascular disease, is considered an inflammatory disease characterized by intense immunological activity in the arteries[2–4]. The circulating monocytes are captured at the surface of endothelium and subsequently roll and extravasate into the aortic intima in the early steps of atherogenesis[5]. Lipids such as low density lipoprotein (LDL) and oxidative LDL, oxidative stress, and inflammatory cytokines activate endothelium and increase the recruitment of monocytes. Extravasated monocytes differentiate into macrophages or dendritic cells. Macrophages, especially the proinflammatory phenotype, M1 macrophages, play an important role in the inflammatory response through their secretion of proinflammatory mediators in the aortic plaque. In the human and mouse aortic plaque, M1 macrophages predominantly exist[5–7]. Inflammatory cytokines induce endothelial dysfunction, stimulate vascular smooth muscle cell migration into the intima and promote atherogenesis.

The prevalence of mild to moderate periodontitis is 13–57% and the prevalence of severe periodontitis is 10–25%[8]. Periodontal disease including periodontitis can affect up to 90% of the worldwide population[9]. Periodontitis is a chronic infectious disease initiated by a group of periodontopathic bacteria, such as *Porphyromonas gingivalis*, which generates lipopolysaccharide (LPS)[10]. LPS activates macrophages through Toll-like receptors and activated macrophages secret inflammatory cytokines. These inflammatory responses induce an imbalance between osteoblasts and osteoclasts and result in alveolar bone absorption[11].

Many prevalent risk factors are shared by cardiovascular disease and periodontal disease, such as age, smoking, diabetes mellitus, and overweight or obesity[12]. Increasing clinical studies have revealed an association between periodontal disease and cardiovascular disease, such as myocardial infarction, stroke and atherosclerotic vascular disease[13–15]. Furthermore, periodontal treatment improves endothelial dysfunction in patients with severe periodontitis[16].

Animal experiments also revealed that *P. gingivalis*-infection accelerated the progression of atherosclerosis in apolipoprotein E-deficient mice[17,18]. Previous reports about rats with ligature-induced periodontitis indicated that periodontitis elicited endothelial dysfunction, oxidative stress and lipid accumulation in aorta accompanied by increased serum inflammatory cytokine, CRP, oxidative stress or lipids[19,20]. Ma *et al.* demonstrated that the

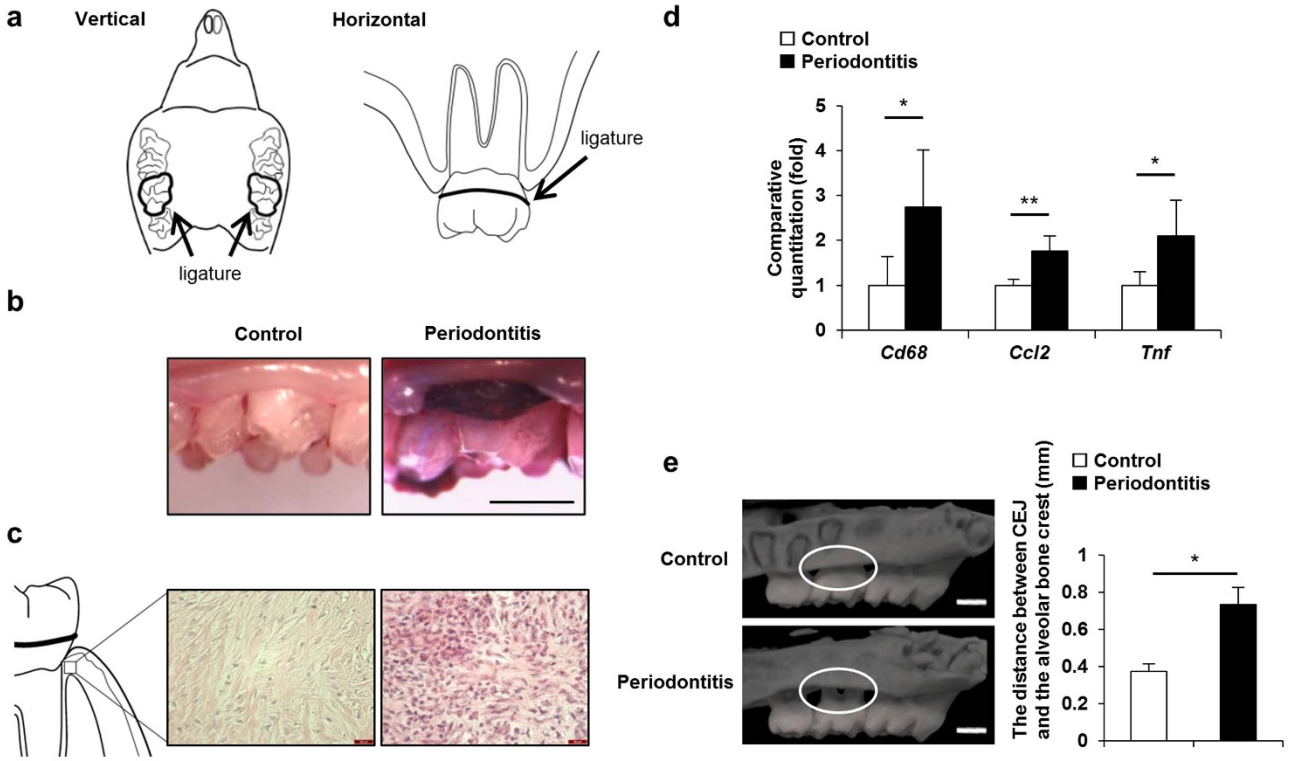

Figure 1 | Induction of periodontitis. (a) Scheme of the ligature around the cervical portion of M2 in the periodontitis rats. (b) Photographs of the cervical portion of the M2 in the control and periodontitis rats 4 weeks after ligature placement. Dental plaque was stained by Red Dye. Scale bar, 1 mm. (c) Ligature-induced periodontitis showed inflammatory cell infiltration in periodontal tissues (hematoxylin and eosin staining). Scale bar, 20 μm. (d) mRNA expression of *Cd68*, *Ccl2* and *Tnf* in gingiva of the control and the periodontitis rats as determined by quantitative RT-PCR ($n = 8$). (e) Micro CT images of maxillae in the periodontitis and the control rats. Bone height was measured as the distance from the mesial buccal cement-enamel junction to the alveolar bone crest of the second molar ($n = 8$). Scale bar, 1 mm. All data represent the means ± s.e.m. $^*P < 0.05$, $^{**}P < 0.01$ in two-sided Student's *t*-test. All schemas were drawing by S. Miyajima.

severity of ligature-induced periodontitis affected the expressions of inflammatory cytokines in aorta[21]. These animal experiments support the epidemiological findings about an association between periodontal disease and cardiovascular disease. Several mechanisms arise from these studies, such as systemic inflammation, molecular mimicry, oxidative stress, lipid abnormality, bacteremia and vascular infection by periodontal pathogens[22]. However, the precise mechanisms by which periodontal disease affects the systemic vasculature remain incompletely defined.

To explore the role of periodontitis in atherosclerosis, we employed an experimental periodontitis model, ligature-induced periodontitis, in rats and investigated the aortic changes thereby induced. Ligature-induced periodontitis is a method to produce an animal model of periodontitis that is similar to clinical periodontitis since it results from plaque accumulation around the ligature[23]. Acute inflammation arises within 2 days post surgery, beginning around the cervical area and leading to a chronic inflammatory response, eventually ending in alveolar bone loss[24–26].

In the current study, we have provided evidence that periodontitis activates monocytes/macrophages, which subsequently circulate in the blood and adhere to vascular endothelial cells inducing an inflammatory response in the vascular wall. Our results indicate that periodontitis triggers the initial pathogenesis of atherosclerosis, the inflammation of the vasculature, through sensitizing circulating monocytes/macrophages.

Results

Induction of periodontitis. We made a ligature-induced periodontitis model which mimics the process of human periodontitis (Fig. 1a). Plaque accumulation was detected around the ligated nylon thread including the dentogingival junction (Fig. 1b). Inflammatory cells were infiltrated in the periodontal tissue of periodontitis rats (Fig. 1c). Inflammatory cytokine mRNA expressions were significantly increased in the gingiva of the periodontitis rats. The gingival *tumor necrosis factor-alpha* (*TNF-α*), *CD68* and *monocyte chemotactic protein-1* (*MCP-1*; also known as *Ccl2*) mRNA expressions significantly increased 2.1-fold, 2.7-fold and 1.7-fold, respectively, in the periodontitis rats compared with the control rats (Fig. 1d).

Alveolar bone resorption was analyzed by the distance between the cemento–enamel junction (CEJ) and the alveolar bone crest (Fig. 1e), which was significantly increased by 1.9-fold in the periodontitis rats compared with the control rats.

Body weights were similar between the control and the periodontitis rats (380.8 ± 15.2 g and 381.6 ± 12.9 g, respectively), whereas the number of white blood cells was significantly higher in the periodontitis rats compared with the control rats (4733 ± 444/μl and 3900 ± 384/μl, respectively, $P < 0.05$).

Periodontitis increased mRNA expressions of TNF-α-associated signal transduction molecules in aorta. We investigated whether periodontitis affected cytokine-related mRNA expressions in the aorta. The induction of periodontitis resulted in the significant increase of TNF-α-related mRNA expressions in the aorta, *TNF-α*, *TNF receptor 1* (*TNFR1*), *TNF receptor-associated factor 2* (*TRAF2*), and *Receptor-interacting protein 1* (*RIP1*; also known as *Ripk1*), as well as the increase of *vascular endothelial adhesion molecules 1* (*VCAM-1*) compared with the control rats, except that there was no significant difference in the *TNF receptor 2* (*TNFR2*) mRNA expression between the control and the periodontitis rats (Fig. 2a).

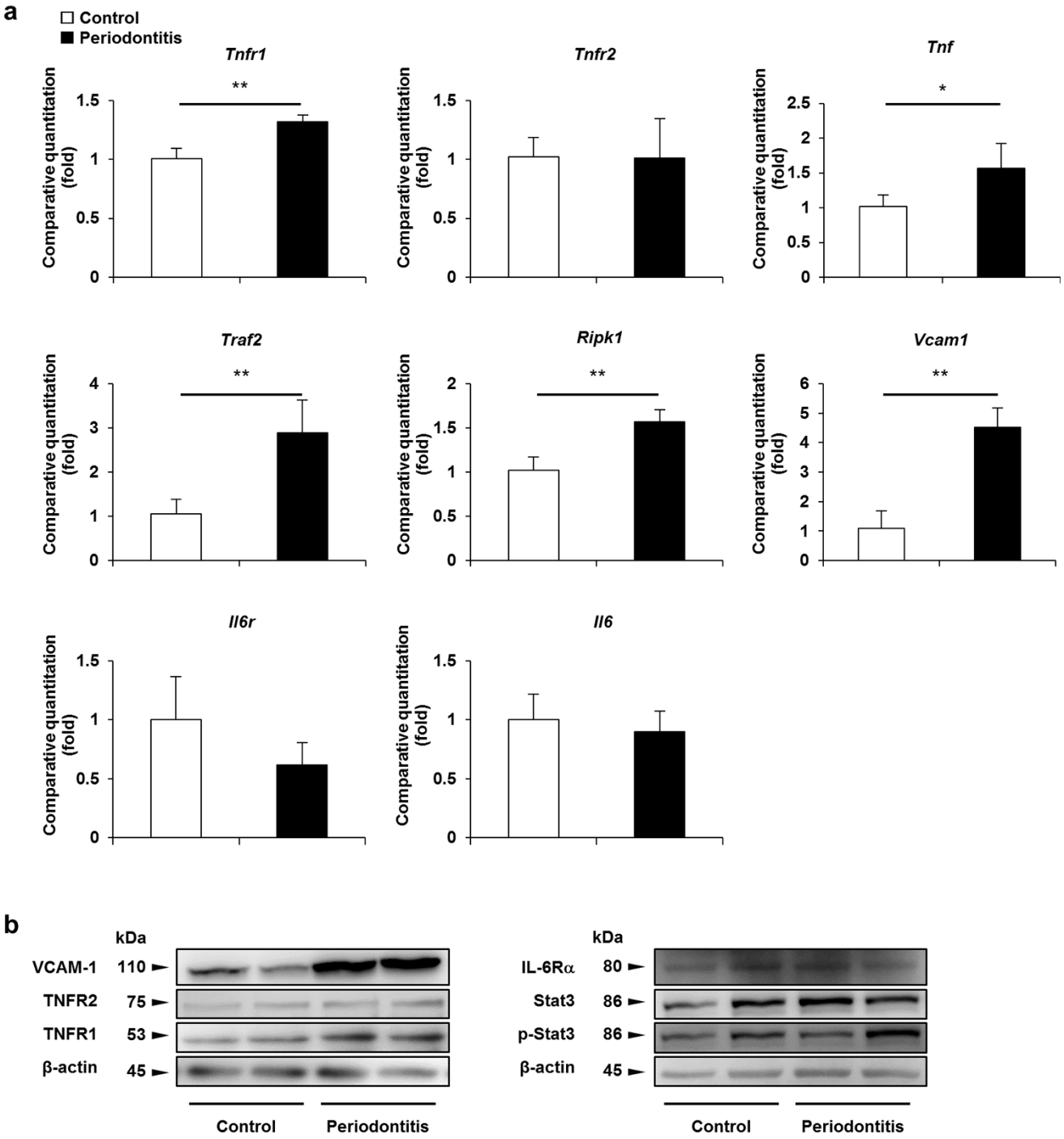

Figure 2 | The effects of periodontitis on mRNA/protein expressions of TNF-α-associated signal transduction molecules in aorta. (a) mRNA expression of *Tnf*, *Tnfr1*, *Tnfr2*, *Traf2*, *Ripk1*, *Il6*, *Il6r* and *Vcam1* in aorta of the control and the periodontitis rats determined by the quantitative RT-PCR (qRT-PCR) ($n = 6$–8). All data represent the means ± s.e.m. $^{*}P < 0.05$, $^{**}P < 0.01$ in two-sided Student's *t*-test. (b) Representative photographs of the protein expressions of TNFR1, TNFR2, VCAM-1, IL-6Rα, p-Stat3, Stat3 and β-actin in aorta of the control and the periodontitis of rats.

Western blot analysis confirmed the increase of the protein expressions of TNFR1 and VCAM-1 in aorta of the periodontitis rats compared with the normal rats (Fig. 2b, Supplementary Fig. S1).

In contrast, mRNA expressions of *interleukin-6* (*IL6*) and its receptor (*IL-6R*) were not changed between the control and the periodontitis rats, which was confirmed by the fact that the protein expression of IL-6Rα and the phosphorylation of Stat3, downstream of IL-6R, were not significantly different in aorta of the control and the periodontitis rats by Western blot analysis (Fig. 2a,b).

Inflammatory cytokines were not increased in serum of the periodontitis rats. The serum concentrations of TNF-α, IL-6, interferon-γ (IFN-γ), MCP-1, and C-reactive protein (CRP) were evaluated. In our rat model, TNF-α, IL-6 and IFN-γ were below the detectable range in both the control and the periodontitis rats (Fig. 3a). MCP-1 was at detectable levels, although there were no differences between the control and the periodontitis rats. Serum CRP concentrations were not different between the control and the periodontitis rats (control; 10.9 ± 0.6 ng/ml, periodontitis; 11.0 ± 0.3 ng/ml). The

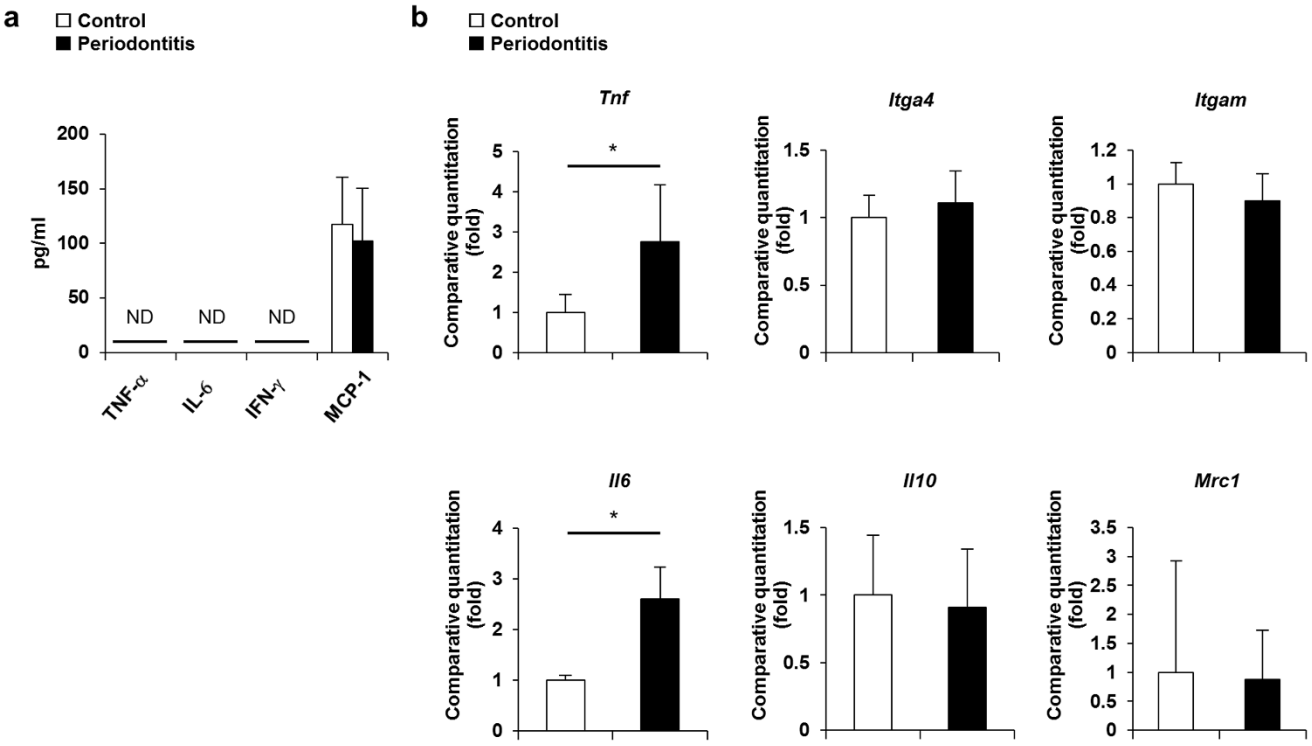

Figure 3 | Effect of periodontitis on serum cytokine levels and mRNA expressions of circulating MNCs. (a) Serum cytokine levels for TNF-α, IL-6, interferon-γ (IFN-γ) and MCP-1 were measured on a multiplex device (Magpix) in the control and periodontitis rats ($n = 8$). ND, not detected. (b) mRNA expressions of *Tnf*, *Itga4*, *Itgam*, *Il6*, *Il10* and *Mrc1* in circulating MNCs from the control and the periodontitis rats. mRNA expressions were determined by quantitative RT-PCR (qRT-PCR) ($n = 5$–7). All data represent the means ± s.e.m. $^*P < 0.05$ in two-sided Student's *t*-test.

tendencies of these results were the same at 2 weeks after ligation (Supplemental Fig.S2).

Effect of periodontitis on the gene expressions in circulating mononuclear cells. To investigate whether circulating mononuclear cells (MNCs) are affected by periodontitis, we collected circulating MNCs from peripheral blood and quantified the mRNA expressions. We measured proinflammatory gene expressions (*TNF-α*, *integrin alpha 4* (*VLA-4*; also known as *Itga4*), *integrin alpha M* (*Mac-1*; also known as *Itgam*) and *IL6*) and anti-inflammatory gene expressions (*interlukin 10* (*IL10*) and *CD206* (also known as *Mrc1*)) (Fig. 3b). The mRNA expression of *TNF-α* and *IL6* were significantly increased by 2.7-fold and 2.6-fold in the MNCs of the periodontitis rats compared to the control rats. On the other hand, there were no significant differences in anti-inflammatory gene expressions. These results indicate that the M1 phenotype of macrophage is activated by periodontitis, suggest that periodontitis-activated MNCs are the inflammatory messenger to the systemic vasculature and that proinflammatory cytokine-related signaling may be involved in the development of vascular dysfunction and atherosclerosis.

Periodontitis increased the adhesion of monocytes/macrophages to aortic endothelial cells. Monocyte accumulation and atherosclerotic lesion formation are known to occur reproducibly at specific sites in the arterial tree, such as in arterial branches[27]. Using an optimal observation method for the endothelial surface, we examined the effect of periodontitis on monocyte/macrophage adhesion to the aortic endothelial surface surrounding the orifice of intercostal arteries of the thoracic aorta in rat (Fig. 4a,b). The number of monocytes/macrophages adhering to the aortic endothelium was significantly increased by 1.7-fold in the periodontitis rats compared with the control rats.

Periodontitis induced NF-κB/VCAM-1 expressions in aortic endothelial cells. Immunohistological stainings revealed that there were significant increases of p65 NF-κB positive and VCAM-1 positive endothelial cells in the aorta of the periodontitis rats compared with the control rats (Fig. 4c,d). Double stainings of these proteins indicated that NF-κB/VCAM-1 double positive endothelial cells were significantly increased in the periodontitis rats, suggesting that NF-κB activation may be involved in the production of VCAM-1 in vascular endothelial cells. These results suggest that periodontitis-activated monocytes/macrophages adhere to aortic endothelial cells, leading to the increase of NF-κB-mediated VCAM-1 expression (Fig. 4e).

Adhesion of peripheral blood-derived MNCs from the periodontitis or the normal rats to cultured vascular endothelial cells. To confirm that circulating monocytes/macrophages in the periodontitis rats have an increased ability to adhere to and induce pathological changes in vascular endothelial cells, we performed ex vivo experiments by collecting MNCs from the periodontitis and the normal rats. MNCs isolated from peripheral blood of the periodontitis or the normal rats were pre-stained by PKH26 and then seeded on a cultured HUVEC monolayer and the number of adhering MNCs was counted. As shown in Fig. 5a,b, the number of MNCs isolated from the periodontitis rats adhering to HUVECs was significantly increased by 3.7-fold compared with those isolated from the control rats.

The adhesion of MNCs from periodontitis rats induced NF-κB activation and VCAM-1 expression in HUVECs, which were significantly increased by 5.1-fold and 2.6-fold, respectively compared with MNCs from the normal rats (Fig. 5c–e).

Discussion

We have demonstrated that periodontitis increases the adhesion of monocytes/macrophages to the aortic endothelium, as well as the activation of NF-κB and the expression of VCAM-1 in aortic endothelial cells using a rat experimental periodontitis model. TNF-

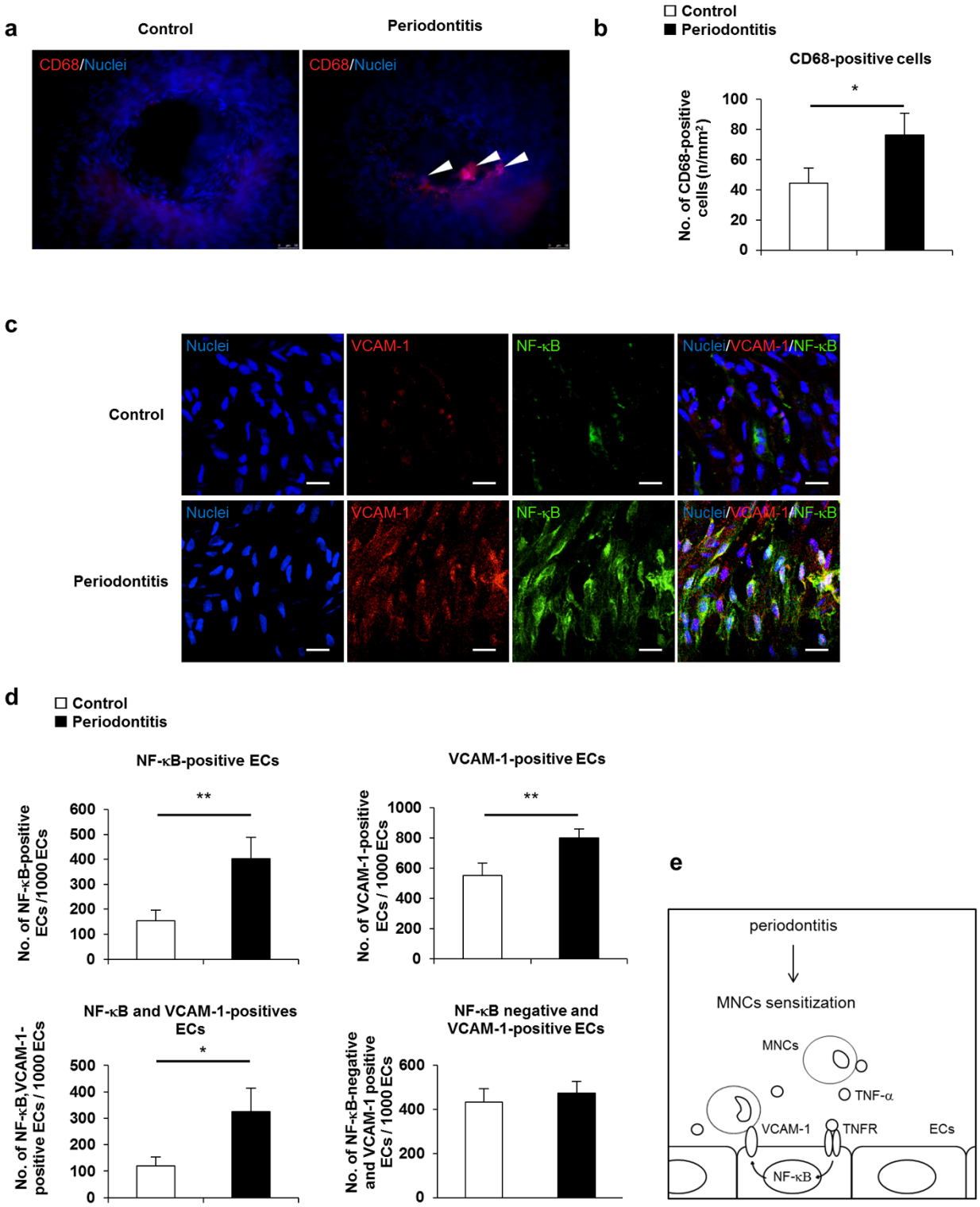

Figure 4 | Effects of periodontitis on monocytes/macropahges adhesion and aortic endothelium. (a) Representative en face views of immunohistochemical staining with CD68 antibody for monocytes adhering to aortic endothelium of the control and the periodontitis rats. Arrowheads denote CD68-positive cells. Scale bar, 50 μm. (b) Quantification of CD68-positive cells ($n = 5$). (c) Representative images of nuclear translocation of p65 NF-κB and VCAM-1 in aortic endothelium of the control and the periodontitis rats. Endothelial cell nuclei, VCAM-1, and p65 NF-κB are in blue, red, and green, respectively. Scale bar, 20 μm. (d) Quantification of endothelial cells positive for nuclear translocation of p65 NF-κB and VCAM-1. $n = 6$ to 8 visual fields. All data represent the means ± s.e.m. $^*P < 0.05$. $^{**}P < 0.01$ in two-sided Student's *t*-test. (e) Possible mechanism involved in periodontitis-sensitized MNCs and their adhesion to endothelial cells.

α receptor cascade, *TNF-α/TNFR1/TRAF2/RIP*, was upregulated in aorta of the periodontitis rats, suggesting that local inflammation, periodontitis, causes an inflammatory response at the sites of the aorta. Our subsequent study indicated that the periodontitis-activated monocytes/macrophages are possible mediators for the induction of the aortic inflammatory response.

Our experimental ligature-induced model of periodontitis is similar to clinical periodontitis since it starts from plaque accumulation

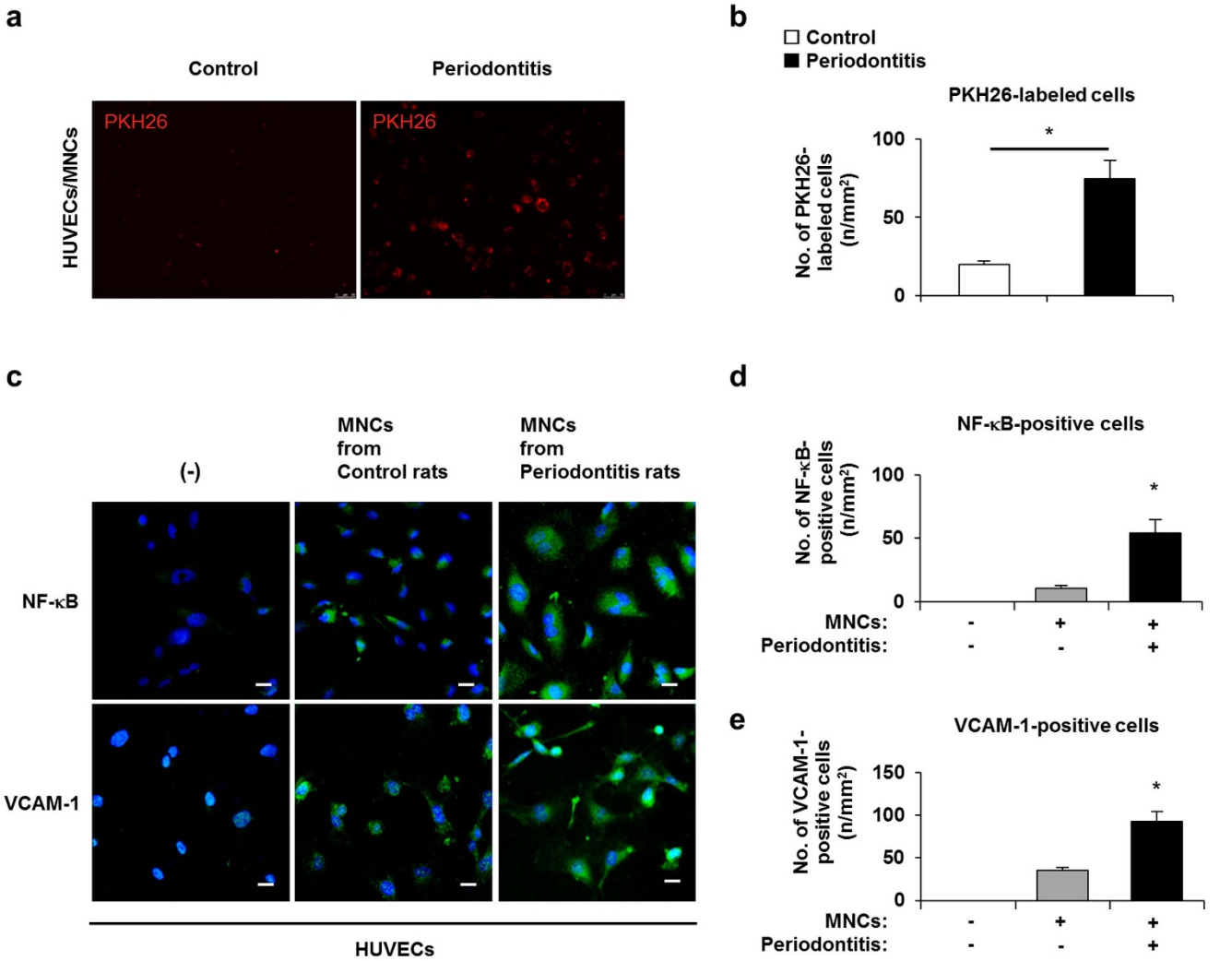

Figure 5 | Effect of periodontitis-activated MNCs on the nuclear translocation of p65 NF-κB and the expression of VCAM-1 in HUVECs. (a) The adhesion of MNCs isolated from peripheral blood of the control and the periodontitis rats to HUVECs. MNCs were labeled with PKH26 and placed on a HUVECs monolayer for 24 h. (b) Quantification of attached PKH26-labeled MNCs ($n = 5$). Scale bar, 50 μm. *$P < 0.05$ in two-sided Student's *t*-test. (c) Representative images of the nuclear translocation of p65 NF-κB and the expression of VCAM-1 in HUVECs. The nuclear translocation of p65 NF-κB was detected 1 h after MNC adhesion and the expression of VCAM-1 was detected 24 h after MNC adhesion, respectively. Endothelial cell nuclei, VCAM-1 and p65 NF-κB are in blue and green, respectively. Scale bar, 20 μm. (d, e) Quantification of HUVECs positive for nuclear translocation of p65 NF-κB and the expression of VCAM-1. $n = 6$ to 8 visual fields. *$P < 0.01$ compared to MNCs from the control rats (by one-way ANOVA). All data represent the means ± s.e.m.

around the ligature, followed by acute inflammation, leading to a chronic inflammatory response and alveolar bone loss[23,26,28]. We evaluated the vascular abnormalities four weeks after ligation, when it was in the chronic inflammatory phase of periodontal disease. Plaque accumulation, inflammatory cell infiltration and alveolar bone loss were observed in the periodontal tissue of the periodontitis rats, as well as the increased expressions of inflammatory cytokines such as TNF-α and MCP-1 in the gingiva.

The adhesion of circulating monocytes to intimal endothelial cells is thought to be one of the earliest events in atherosclerogenesis[2,29]. Subsequently, monocytes attached to endothelial cells invade the vascular wall and play a pivotal role in the inflammatory response in the vasculature[30]. Thus, our results indicate that periodontitis induces an early event of atherosclerogenesis, monocyte adhesion to aortic endothelium.

Immunohistological staining revealed that the expressions of NF-κB and VCAM-1 were significantly increased in the aortic endothelial cells of rats with periodontitis. Endothelium-expressed adhesion molecules, such as VCAM-1 and ICAM-1, have pathogenic functions during atherosclerogenesis[31]. They may also contribute to the initiation lesions by participating in the recruitment of blood monocytes to the intima in the earliest stages of atherosclerosis. The induction of VCAM-1 at sites of atherosclerotic lesion formation is an example of inducible NF-κB-dependent gene expression during the formation of early atherosclerotic lesions, since the promoter of VCAM-1 contains two consensus NF-κB sites that are required for cytokine-induced expression[27,32].

Periodontitis increased the mRNA expressions of TNF-α receptor cascade, *TNF-a/TNFR1/TRAF2/RIP* as well as VCAM-1 in the aorta. The members of the TNF ligand family exert their biological functions via interaction with their cognate membrane receptors, comprising the TNF receptor (TNF-R) family[33]. Although TNFR2 can directly bind TRAF2 (as well as TRAF1), it does not activate the expression of adhesion molecules in endothelial cells[34]. On the other hand, the TNFR1-mediated cascade induces the activation of NF-κB[35]. TNF stimulation of adhesion molecules, ICAM-1 and VCAM-1, in human endothelial cells occurs through the TNFR1 subtype and is mediated by the NF-κB pathway, but not the ERK, p38MAPK or

JNK kinase pathways. It is also evident from studies with TRADD-, TRAF2- and RIP1-deficient mice that all these molecules play important roles in the TNFR1-induced activation of NF-κB[36,37]. In contrast, Ekuni et al. reported that other gene expressions were increased in aorta of ligature-induced periodontitis Wistar rats by microarray analysis, and that TNF-α was not increased in their model. At least, both two studies indicated that ligature-induced periodontitis changed the gene profiles in aorta. The reason for the differences in gene profiles between them is unknown, but one possibility is differences in the rat lineages. Concerning this issue, further study is needed.

In contrast with TNF-α signaling cascade, IL-6 signaling cascade was not increased in aorta of the periodontitis rats. The mRNA expressions of IL-6 and IL-6R, the protein levels of IL-6R and the phosphorylation of Stat3, downstream of IL-6R, were not significantly different in aorta between the control and the periodontitis rats.

What is the mediator between periodontitis and the aortic inflammatory changes in our model? The serum levels of inflammatory cytokines were undetectable or unchanged between the control and the periodontitis rats in our experiments, suggesting that serum cytokines may not be the inducer of aortic inflammation. On the other hand, we have demonstrated that the circulating MNCs including monocytes/macrophages showed a significant increase in TNF-α and IL-6 mRNA expression in the periodontitis rats compared with the control rats.

Our *ex vivo* experiments revealed that peripheral blood-derived MNCs from periodontitis rats had enhanced adhesion to vascular endothelial cells compared with those from the control rats. We also confirmed that MNCs from the periodontitis rats significantly increased the expressions of NF-κB and VCAM-1 in cultured vascular endothelial cells compared with those from the control rats. These results suggest that circulating MNCs activated by periodontitis become more strongly adhesive to vascular endothelial cells, which subsequently induce the inflammatory response in the vascular wall.

Previous studies demonstrated that ligature-induced periodontitis increased serum oxidative stress and LDL-cholesterol in rats[19,20]. Clinical studies revealed that the severity of periodontitis positively correlated with serum oxidative stress[38,39]. Although we did not measure oxidative stress or lipids profiles in our study, oxidative stress is known to induce the activation of monocytes/macrophages[40,41]. These facts may suggest that the monocytes/macrophages were activated not only at the sites of periodontitis but also in the serum by oxidative stress. Concerning this issue, further validation is needed.

In conclusion, to our knowledge, this is the first study, using a ligature-induced periodontitis method, which directly demonstrated that periodontitis induces inflammatory changes in the vascular wall, at least in part through activated monocytes/macrophages. These results indicate the importance of the treatment of periodontal disease in the aspect of preventing atherosclerosis. We endorse the treatment of periodontal disease not only for treating the local infection but also for preventing the aortic inflammation.

Methods

Animals. Male Sprague-Dawley (SD) rats were purchased from Chubu Kagakushizai (Nagoya, Japan) at 7 weeks of age. All rats were housed in individual cages under controlled temperature (24 ± 1.0°C), on a 12 h light/dark cycle and were given standard laboratory rat chow with water ad libitum. All experimental protocols were approved by the Institutional Animal Care and Use Committees of Aichi Gakuin University and all experiments were carried out in accordance with the approved guidelines.

Induction of periodontitis. Periodontitis was induced in rats by nylon thread ligature as previously described[42]. Half of the rats, the periodontitis rats, were anesthetized with diethyl ether, and surgical nylon thread (3-0 Surgilon; Tyco Healthcare, Princeton, NJ) was used to ligate around the cervical portion of the maxillary second molar (M2) on both sides without damaging the nearby gingiva. Rats without any ligation were used as the control rats. Four weeks after the ligature, the following assessments were performed.

Tissue collection. Rats were killed with an overdose of pentobarbital and blood samples were collected from the central vein. An approximately 3 mm thick gingivomucosal tissue strip from the buccal side of the M2 was excised from the left side and kept at −80°C until use for mRNA and protein analyses. Maxillary bones with the attached gingival tissue from the right side were excised and fixed in 10% formalin for H-E staining and micro CT analyses. The gingivomucosal and maxilla samples of all rats were removed by the same investigator. The aorta was harvested, immediately frozen and kept at −80°C until processed for mRNA/protein analyses or fixed with 4% paraformaldehyde for immunohistochemical analysis.

Dental plaque-disclosing. To detect the plaque accumulation on the tooth surface, Red Dye (Merssage®; Shofu, Kyoto, Japan) was used according to the manufacturer's protocol[43]. Red Dye was applied to all exposed tooth surfaces, followed by rinsing with deionized water. The plaque on the teeth remained red after the rinsing.

Real-time quantitative RT-PCR. Total RNA was extracted using RNeasy (Qiagen, Hilden, Germany) and complementary DNA was synthesized from 250 ng of RNA using ReverTra Ace (Toyobo, Osaka, Japan) according to the manufacturers's instructions. Primers were purchased from TaqMan Gene Expression Assays (Applied Biosystems, Foster City, CA). Real-time quantitative PCR was performed using ABI Prism 7000 (Applied Biosystems). The following protocol was used: 1 min. at 95°C, 1 min. at 52°C and 30 s at 72°C, and it was repeated for a total of 40 cycles. The relative quantity was calculated by the ΔΔCT method using β2 microglobulin as the endogenous control[44].

Micro CT analysis. To observe the morphological changes in the alveolar bone, maxilla were scanned by micro CT (R_mCT; Rigaku Corporation, Tokyo, Japan) 4 weeks after ligature. The computed tomography was set according to slice thickness (50 um), voltage (90 kV) and electrical current (88 mA). Three-dimensional images were made using TRI/3D Bone (Ratoc, Tokyo, Japan). The distance from the mesial buccal cement-enamel junction to the alveolar bone crest of the second molar was measured as a reference for bone height. The level of bone resorption was calculated as the distance from the mesiobuccal cement-enamel junction to the alveolar bone crest.

Western blot analysis. Frozen, powdered samples of aorta were solubilized in lysis buffer and analyzed by Western blot using antibodies to rabbit anti-TNFR1 polyclonal antibody, rabbit anti-TNFR2 polyclonal antibody, rabbit anti-VCAM-1 polyclonal antibody mouse anti-IL-6Rα monoclonal antibody (Santa Cruz Biotechnology Inc, Santa Cruz, CA), mouse anti-Stat3 monoclonal antibody, mouse anti-β-actin monoclonal antibody (Cell Signaling Technologies, Beverly, MA). The expression of β-actin was used to control for equal gel loading.

Histological and immunofluorescence staining in gingiva and aorta. Maxilla with gingiva on both sides were fixed in 10% formalin solution for 24 hours, washed in tap water and immersed in a specific immersing solution (SCEM) containing liquid nitrogen and isopentane. Following this procedure, undecalcified frozen sections were made according to the Kawamoto method[45]. For hematoxylin-eosin staining, the second molars were cut serially into 5-μm-thick sections, the sections then mounted using adhesive film (Cryofilm type I; Laica microsystems,Wetzlar, Germany) and mounting medium (SCMM-R2; Laica microsystems).

The accumulation of monocytes/macrophages on the endothelial surface and en face immunohistochemistry of the endothelial surface were observed using a combination of inverted fluorescent microscopy and confocal microscopy. The aorta was dissected carefully from the aortic arch to the lower thoracic region and was immersed in 4% paraformaldehyde for 24 hours at 4°C. The thoracic aorta, which was cleamed of fat for en face immunohistochemistry of the endothelial surface, was cut open longitudinally along the ventral side with scissors. Then, immunohistochemical analysis was performed using anti-rabbit VCAM-1 antibody (Santa Cruz Biotechnology Inc), anti-human NF-κB (p65) antibody (Life Technologies Corp., Carlsbad, CA) or anti-mouse CD 68 monoclonal antibody (Thermo Fisher Scientific, Cheshire, UK). This was followed by incubation with the secondary antibodies labeled with Alexa Fluor 488, 594 or Texas Red (Life Technologies Corp.) and with DAPI (Sigma-Aldrich, St. Louis, MO) for 1 hour at room temperature. The samples were washed 3 times with PBS, placed on a slide glass with the intimal side up, and covered with Fluormount (Diagnostic BioSystems, Pleasanton, CA) Mounting Medium. Slides were investigated with a FU-200 confocal system (Olympus, Tokyo, Japan) and Leica AF6000LX (Leica microsystems) inverted microscope. To count the number of endothelium-adherent monocytes, the total numbers of CD 68-immunopositive cells were counted and the cell density was calculated as the cell count divided by the total area[46]. The activation of NF-κB was detected by immunofluorescent staining of NF-κB in or near the nuclei. Seven to ten fields were captured at various focal lengths and the ratio of NF−κB positive and VCAM-1 positive cells was determined as positive cells per 1000 endothelial cells[47].

Serum cytokine measurements. Serum concentrations of TNF-α, IL-6, IFN-γ, and MCP-1were measured using multiple beads array (Milliplex MAP kit, Millipore Corp, Billerica, MA) following the manufacturer's instructions and the concentrations of the analytes were determined in the serum collected from rats using Milliplex Manager version 5.1 and MAGPIX xPONENT software, respectively. The serum concentration of CRP was measured by ELISA (R&D Systems, Minneapolis, MN, USA). All samples were run in triplicate. Analytes were normalized to the total protein concentration, which was estimated with a Bradford assay, a colorimetric protein assay.

Isolation and labeling of MNCs. MNCs were isolated from peripheral blood using the Histopaque (Sigma)-density centrifugation method. The MNCs layer was collected, washed twice with 1 mmol/l EDTA in PBS, and suspended in degassed PBS with 0.5% BSA and 2 mmol/l EDTA. After the removal of platelets and red blood cells, MNCs were stained with PKH26-GL Red Fluorescent Cell Linker Kit (Sigma) and Hoechst 33342 (Life Technologies Corp.) according to the manufacturer's protocol.

***Ex vivo* adhesion of circulating MNCs to cultured endothelial cells and immunohistochemical staining of endothelial cells co-cultured with MNCs.** 1×10^5 MNCs were labeled with PKH26 (Sigma), placed on a confluent human umbilical vein endothelial cells (HUVECs) (Lonza, Walkersville, MD) monolayer in each well of a 4-well chamber slide (Iwaki, Tokyo, Japan) and allowed to adhere for 1 and 24 hours. Nonadherent cells were washed away and the cells were fixed with 4% paraformaldehyde; the number of labeled adherent MNCs was determined by counting cells in five 100 × fields per well[48,49].

For the immunohistological staining of endothelial cells cultured with attached MNCs, after the fixation, cells were incubated 1 hour at 4°C with PBS containing anti-rabbit VCAM-1 antibodies (Santa Cruz Biotechnology Inc), anti-human NF-κB (p65) antibodies (Life Technologies Corp.), followed by species-specific secondary antibodies coupled with Alexa Fluor Dyes (Life Technologies Corp.). Nuclei were stained using Hoechst 33342, and the cells were mounted in Fluormount (Diagnostic BioSystems, Pleasanton, CA) Mounting Medium for imaging with a FU-200 confocal system (Olympus). 5 to 7 pictures of each field were captured at various focal lengths and positive cells were counted in 100 × fields per well.

Statistical analyses. Data are expressed as means ± s.e.m. Differences between two groups were assessed using the unpaired two-tailed Student's *t*-test unless otherwise noted. Data sets involving more than two groups were assessed by analysis of variance (one-way ANOVA) followed by the Bonferroni correction for multiple comparisons. The differences were considered to be significant if $P < 0.05$.

1. Alwan, A. *Global status report on noncommunicable diseases 2010*. World Health Organization (2011).
2. Ross, R. Atherosclerosis-an inflammatory disease. *N Engl J Med* **340**, 115–126 (1999).
3. Libby, P. Inflammation in atherosclerosis. *Nature* **420**, 868–874 (2002).
4. Hansson, G. K. & Libby, P. The immune response in atherosclerosis: a double-edged sword. *Nat Rev Immunol* **6**, 508–519 (2006).
5. Moore, K. J., Sheedy, F. J. & Fisher, E. A. Macrophages in atherosclerosis: a dynamic balance. *Nat Rev Immunol* **13**, 709–721 (2013).
6. Bessaad, A. *et al.* M1-activated macrophages migration, a marker of aortic atheroma progression: a preclinical MRI study in mice. *Invest Radiol* **45**, 262–269 (2010).
7. Cho, K. Y. *et al.* The phenotype of infiltrating macrophages influences arteriosclerotic plaque vulnerability in the carotid artery. *J Stroke Cerebrovasc Dis* **22**, 910–918 (2013).
8. Rylev, M. & Kilian, M. Prevalence and distribution of principal periodontal pathogens worldwide. *J Clin Periodontol* **35**, 346–361 (2008).
9. Pihlstrom, B. L., Michalowicz, B. S. & Johnson, N. W. Periodontal diseases. *Lancet* **366**, 1809–1820 (2005).
10. Wang, P. L. & Ohura, K. *Porphyromonas gingivalis* lipopolysaccharide signaling in gingival fibroblasts-CD14 and Toll-like receptors. *Crit Rev Oral Biol Med* **13**, 132–142 (2002).
11. Graves, D. T. & Cochran, D. The contribution of interleukin-1 and tumor necrosis factor to periodontal tissue destruction. *J Periodontol* **74**, 391–401 (2003).
12. Hujoel, P. P., Drangsholt, M., Spiekerman, C. & DeRouen, T. A. Periodontal disease and coronary heart disease risk. *JAMA* **284**, 1406–1410 (2000).
13. Arbes, S. J. Jr., Slade, G. D. & Beck, J. D. Association between extent of periodontal attachment loss and self-reported history of heart attack: an analysis of NHANES III data. *J Dent Res* **78**, 1777–1782 (1999).
14. Holmlund, A., Holm, G. & Lind, L. Number of teeth as a predictor of cardiovascular mortality in a cohort of 7,674 subjects followed for 12 years. *J Periodontol* **81**, 870–876 (2010).
15. Humphrey, L. L., Fu, R., Buckley, D. I., Freeman, M. & Helfand, M. Periodontal disease and coronary heart disease incidence: a systematic review and meta-analysis. *J Gen Intern Med* **23**, 2079–2086 (2008).
16. Tonetti, M. S. *et al.* Treatment of periodontitis and endothelial function. *N Engl J Med* **356**, 911–920 (2007).
17. Li, L., Messas, E., Batista, E. L. Jr., Levine, R. A. & Amar, S. *Porphyromonas gingivalis* infection accelerates the progression of atherosclerosis in a heterozygous apolipoprotein E-deficient murine model. *Circulation* **105**, 861–867 (2002).
18. Lalla, E. *et al.* Oral infection with a periodontal pathogen accelerates early atherosclerosis in apolipoprotein E-null mice. *Arterioscler Thromb Vasc Biol* **23**, 1405–1411 (2003).
19. Brito, L. C. *et al.* Experimental periodontitis promotes transient vascular inflammation and endothelial dysfunction. *Arch Oral Biol* **58**, 1187–1198 (2013).
20. Ekuni, D. *et al.* Effects of periodontitis on aortic insulin resistance in an obese rat model. *Lab Invest* **90**, 348–359 (2010).
21. Batty, G. D. *et al.* Oral disease in relation to future risk of dementia and cognitive decline: prospective cohort study based on the Action in Diabetes and Vascular Disease: Preterax and Diamicron Modified-Release Controlled Evaluation (ADVANCE) trial. *Eur Psychiatry* **28**, 49–52 (2013).
22. Lockhart, P. B. *et al.* Periodontal disease and atherosclerotic vascular disease: does the evidence support an independent association?: a scientific statement from the American Heart Association. *Circulation* **125**, 2520–2544 (2012).
23. Rovin, S., Costich, E. R. & Gordon, H. A. The influence of bacteria and irritation in the initiation of periodontal disease in germfree and conventional rats. *J Periodontal Res* **1**, 193–204 (1966).
24. de Souza, J. A. C., Nogueira, A. V. B., de Souza, P. P. C., Cirelli, J. A., Garlet, G. P. & Rossa, Jr. C. Expression of suppressor of cytokine signaling 1 and 3 in ligature-induced periodontitis in rats. *Arch Oral Biol* **56**, 1120–1128 (2011).
25. Soboku, K. *et al.* Altered gene expression in gingival tissues and enhanced bone loss in diabetic rats with experimental periodontitis. *J Periodontol* **85**, 455–464 (2014).
26. Tomofuji, T. *et al.* Preventive effects of a cocoa-enriched diet on gingival oxidative stress in experimental periodontitis. *J Periodontol* **80**, 1799–1808 (2009).
27. Iiyama, K. *et al.* Patterns of vascular cell adhesion molecule-1 and intercellular adhesion molecule-1 expression in rabbit and mouse atherosclerotic lesions and at sites predisposed to lesion formation. *Circ Res* **85**, 199–207 (1999).
28. Kennedy, J. E. & Polson, A. M. Experimental marginal periodontitis in squirrel monkeys. *J Periodontol* **44**, 140–144 (1973).
29. Cybulsky, M. I. *et al.* A major role for VCAM-1, but not ICAM-1, in early atherosclerosis. *J Clin Invest* **107**, 1255–1262 (2001).
30. Kavurma, M. M. & Bennett, M. R. Expression, regulation and function of trail in atherosclerosis. *Biochem Pharmacol* **75**, 1441–1450 (2008).
31. Walker, L. N., Reidy, M. A. & Bowyer, D. E. Morphology and cell kinetics of fatty streak lesion formation in the hypercholesterolemic rabbit. *Am J Pathol* **125**, 450–459 (1986).
32. Collins, T. & Cybulsky, M. I. NF-kappaB: pivotal mediator or innocent bystander in atherogenesis? *J Clin Invest* **107**, 255–264 (2001).
33. Locksley, R. M., Killeen, N. & Lenardo, M. J. The TNF and TNF receptor superfamilies: integrating mammalian biology. *Cell* **104**, 487–501 (2001).
34. Slowik, M. R., De Luca, L. G., Fiers, W. & Pober, J. S. Tumor necrosis factor activates human endothelial cells through the p55 tumor necrosis factor receptor but the p75 receptor contributes to activation at low tumor necrosis factor concentration. *Am J Pathol* **143**, 1724–1730 (1993).
35. Zhou, Z., Connell, M. C. & MacEwan, D. J. TNFR1-induced NF-kappaB, but not ERK, p38MAPK or JNK activation, mediates TNF-induced ICAM-1 and VCAM-1 expression on endothelial cells. *Cell Signal* **19**, 1238–1248 (2007).
36. Ermolaeva, M. A. *et al.* Function of TRADD in tumor necrosis factor receptor 1 signaling and in TRIF-dependent inflammatory responses. *Nat Immunol* **9**, 1037–1046 (2008).
37. Pobezinskaya, Y. L. *et al.* The function of TRADD in signaling through tumor necrosis factor receptor 1 and TRIF-dependent Toll-like receptors. *Nat Immunol* **9**, 1047–1054 (2008).
38. Baltacioglu, E. *et al.* Total oxidant status and bone resorption biomarkers in serum and gingival crevicular fluid of patients with periodontitis. *J Periodontol* **85**, 317–326 (2014).
39. Tamaki, N. *et al.* Oxidative stress and antibody levels to periodontal bacteria in adults: the Nagasaki Islands study. *Oral Dis* **20**, e49–56 (2014).
40. Gamaley, I. A., Kirpichnikova, K. M. & Klyubin, I. V. Activation of murine macrophages by hydrogen peroxide. *Cell Signal* **6**, 949–957 (1994).
41. Tang, D. *et al.* Hydrogen peroxide stimulates macrophages and monocytes to actively release HMGB1. *J Leukoc Biol* **81**, 741–747 (2007).
42. Nishikawa, T. *et al.* Involvement of nitrosative stress in experimental periodontitis in diabetic rats. *J Clin Periodontol* **39**, 342–349 (2012).
43. O'Leary, T. J., Drake, R. B. & Naylor, J. E. The plaque control record. *J Periodontol* **43**, 38 (1972).
44. Livak, K. J. & Schmittgen, T. D. Analysis of relative gene expression data using real-time quantitative PCR and the 2(-Delta Delta C(T)) Method. *Methods* **25**, 402–408 (2001).
45. Kawamoto, T. Use of a new adhesive film for the preparation of multi-purpose fresh-frozen sections from hard tissues, whole-animals, insects and plants. *Arch Histol Cytol* **66**, 123–143 (2003).
46. Azuma, K. *et al.* A new En face method is useful to quantitate endothelial damage in vivo. *Biochem Biophys Res Commun* **309**, 384–390 (2003).
47. Yamada, H. *et al.* In vivo and in vitro inhibition of monocyte adhesion to endothelial cells and endothelial adhesion molecules by eicosapentaenoic acid. *Arterioscler Thromb Vasc Biol* **28**, 2173–2179 (2008).
48. Imai, T. *et al.* Identification and molecular characterization of fractalkine receptor CX3CR1, which mediates both leukocyte migration and adhesion. *Cell* **91**, 521–530 (1997).
49. Kawakami, A., Aikawa, M., Alcaide, P., Luscinskas, F. W., Libby, P. & Sacks, F. M. Apolipoprotein CIII induces expression of vascular cell adhesion molecule-1 in vascular endothelial cells and increases adhesion of monocytic cells. *Circulation* **114**, 681–687 (2006).

Acknowledgments

This research was supported in part by Grant-in-Aid for Scientific Research (22592322) from the Ministry of Education, Culture, Sports, Science and Technology (MEXT) and in

part by the "Strategic Research AGU-Platform Formation (2008–2012)" Project for Private Universities: matching fund subsidy from MEXT of Japan.

Author contributions

K.N. conceived and designed the research. S.M. performed the experiments and wrote the manuscript with the help of Y.K., K.A. and Y.S., T.N. and T.K. established the ligature-induced periodontitis. N.N. performed en face immunohistochemistry of the aortic surface. M.M. and N.O. performed histological assessments. A.M., T.N. and T.M. supervised the project. We thank Mr. Brent Bell for reading the manuscript.

Additional information

Supplementary information accompanies this paper at http://www.nature.com/scientificreports

Competing financial interests: The authors declare no competing financial interests.

How to cite this article: Miyajima, S. *et al.* Periodontitis-activated monocytes/macrophages cause aortic inflammation. *Sci. Rep.* **4**, 5171; DOI:10.1038/srep05171 (2014).